FRACTURE TOUGHNESS OF THIN NODULAR CAST IRON

Michael Janssen* and Hans Boone*

The *J-R* curve is determined for nodular cast iron with wall thicknesses ranging from 2 to 7 mm. The nodules in these materials differ in size and relative distance and an effect on fracture toughness can be expected.

For 2 mm material, the standard *J-R* test method prescribes SENB specimens with such small dimensions that accurate tests cannot be performed. Therefore, experiments are carried out on SENT specimens and the results are compared to those obtained using standard specimens.

The results indicate that fracture toughness of the cast iron decreases as the thickness decreases. This effect can be related to the nodule morphology, using a fracture model for the CTOD required for void growth and coalescence. Furthermore, the use of SENT specimens is found to enable *J-R* curve determination on 2 mm specimens

INTRODUCTION

Recent developments have enabled the production of thin-walled (≈ 2 mm) nodular cast iron. This material contains a large number of small-sized nodules. Structural automotive application for this material, traditionally the domain for thin aluminium and steel plate, requires knowledge of the fracture toughness.

Due to the thinness of this type of nodular cast iron in combination with its ductility, the plane-strain fracture toughness K_{Ic} can not be determined. For this reason it was decided to quantify fracture toughness by determining the *J-R* curve. The main objective of this research is to quantify the *J-R* curve of the cast iron as a function of the nodule morphology, i.e. nodule size and nodule spacing. These differences in morphology are obtained by using cast iron with three different wall thicknesses, i.e. 7, 4 and 2 mm.

Although the most recent standard on *J-R* testing is ASTM E 1737-96, the present work is based on the somewhat older ASTM standard E 1152-95 (1). For 2 mm thick material, this standard prescribes very small dimensions for Single Edge Notched Bending (SENB) specimens. This hampers the accurate measurement of load-line displacement and compliance, necessary for determining *J* and the amount of stable crack growth respectively. For this reason the non-standardised Single Edge Notched Tensile (SENT) geometry is considered for evaluating the *J-R* curve.

* Laboratory for Materials Science, Delft University of Technology, The Netherlands

For the present study *J-R* test are performed on 7 and 4 mm thick SENB specimens according to ASTM standard E 1152-95. Furthermore, experiments are performed on 4 and 2 mm thick SENT specimens, this time using the modified *J*-integral, J_M, originally introduced by Ernst (4). One of the reasons is, that for the SENT geometry, only the solution for J_M is available. Furthermore, Landes et al (3) suggest that possible geometry effects are smaller when J_M is used. For the SENB results J_M is calculated also, thereby enabling a comparison between the results on the 4 mm SENB and SENT specimens.

J-R CURVE DETERMINATION

A *J-R* curve for a material is determined by loading a fatigue pre-cracked specimen in such a way that stable crack growth occurs. During the test the applied load *P* and the load-line displacement δ are recorded. Furthermore, the amount of stable crack growth needs to be measured. In case of a single specimen test this can be done by means of the unloading compliance technique: at discrete intervals the elastic compliance *C*, i.e. the ratio between crack mouth opening displacement (CMOD) and the load, is measured and afterwards the corresponding crack extension is calculated.

Standard *J* determination. The *J*-integral used in the ASTM-standard is based on deformation theory of plasticity. Its value at any point during the test can be calculated using the instantaneous values of any two out of the three variables crack length *a*, load *P*, and displacement δ. Furthermore, J_D does not depend on the path followed in P-δ-a space to reach the current state (2). However, the most obvious path for evaluating *J* is the P-δ test record itself. For bend type specimens (CT and SENB) *J* follows from (2):

$$J = \int_0^{\delta} \frac{\eta}{Bb} P \, d\delta - \int_{a_0}^{a} \frac{\gamma}{b} J \, da \ , \qquad (1)$$

where γ and η are work factors depending on geometry and possibly crack size, a_0 is the initial crack length, and *B* and b are specimen thickness and ligament size respectively. This equation leads to the approximate incremental formulation for *J*, which was eventually included in the ASTM standard (1). In this standard, although not strictly necessary, *J* is divided into an elastic part, i.e. the linear elastic energy release rate *G*, and a plastic part $J_{pl} = J - G$. To calculate J_{pl}, the plastic part of the load-line displacement, δ_{pl}, is used, which simply is the total displacement δ minus the elastic part $\delta_{el} = C_{LL} \cdot P$, where C_{LL} is the elastic load-line compliance. The resulting incremental expression for J_{pl} is:

$$J_{pl(i)} = \left[J_{pl(i-1)} + \frac{\eta_i}{Bb_i} A_{i-1,i}\right]\left[1 - \frac{\gamma_i}{b_i}(a_i - a_{i-1})\right] \ , \qquad (2)$$

where $A_{i-1,i}$ is the area under the P-δ curve between displacements δ_i and δ_{i-1}.

Determination of modified *J*. The modified *J* was originally defined by Ernst (4) as:

$$J_M = J - \int_{a_0}^{a} \left(\frac{\partial J_{pl}}{\partial a}\right)_{\delta_{pl}} da = G + \int_0^{\delta_{pl}} \left(\frac{\partial J_{pl}}{\partial \delta_{pl}}\right)_a d\delta_{pl} \ . \qquad (3)$$

The second expression can be derived by considering J_{pl} as a differentiable function of *a* and δ_{pl}. The modified *J* is history dependent and deviates more from *J* as (i) the amount of stable crack extension relative to the ligament *b* becomes larger and (ii) the material is tougher. Writing J_{pl} for a non-growing crack as:

$$J_{\mathrm{pl}} = \frac{\eta}{Bb}\int_{0}^{\delta_{\mathrm{pl}}} \mathrm{P}\,\mathrm{d}\delta_{\mathrm{pl}} \;, \tag{4}$$

J_{M} can be written as:

$$J_{\mathrm{M}} = G + \int_{0}^{\delta_{\mathrm{pl}}} \frac{\eta}{Bb}\mathrm{P}\,\mathrm{d}\delta_{\mathrm{pl}} \;. \tag{5}$$

Work factors. For the SENB specimens used in the current research $\eta = 2.0$ and $\gamma = 1.0$ (1). For the SENT geometry, the calculations are based on an η-value of 1.9 (3).

Crack length determination. For the SENB specimens the crack length is measured using the unloading compliance technique described in ASTM standard E 1152-95 (1). In addition, the measured compliances are corrected for crack front tunnelling, specimen deformation and friction at- and movement of the rollers, all according to reference (2). For the SENT specimens, the unloading compliance technique is applied also, now based on the compliance data given by Tada (5).

EXPERIMENTAL

Material data. The cast iron contains about 3.8% C, 2.9% Si, 0.04% Mn, and 0.6% Ni. In Table 1 an overview is given of the number of nodules per area, the average nodule spacing and the nodule diameter. In Figure 1 the metallographic structures of the 7, 4 and 2 mm thick nodular cast iron are shown.

TABLE 1 – Nodule morphology of the nodular cast iron

Thickness [mm]	Nodules per mm^2	Nodule spacing [μm]	Nodule size [μm]
2	5500 - 7200	16	14
4	1300 - 1650	30	18
7	400-650	54	32

Specimen Geometry. The SENB geometry complies with the ASTM standard (1), albeit that a width-to-thickness ratio of 4 is chosen to facilitates the compliance determination for the relatively small specimens. The SENT geometry is depicted in Figure 2 and is derived from the geometry used by Landes et al (3).

RESULTS AND DISCUSSION

Crack length from compliance. The crack front curvature in the SENB specimens was found to amply exceed the amount permissible according to the ASTM standard. In spite of this, correcting the measured compliance according to (2) yielded a total crack extension that in all cases was within 15% of the measured physical crack extension.

For the SENT specimens compliance data were not corrected. The crack extensions calculated for the 4 mm thick specimens agreed within 15% with the measured physical values. However for the 2 mm thick specimens this was not the case. It should be noted, however, that the fracture surfaces of all SENT specimens showed a peculiar phenomenon: areas were present with a slightly different colouring. This was especially so along the specimen surfaces. It is not clear whether this phenomenon was due to crack front tunnelling or to an irregular shape of the surface of the stable crack extension. By measuring the physical crack extension for the 2 mm specimens, while excluding these areas, the crack extensions calculated from compliance did agree within 15%.

J_M-R curves. In Figures 3 and 4 the average J-R respectively J_M-R curves for the SENB specimens are presented in the form of power-law fits. The 95% reliability intervals are shown also. These results are based on 11 tests on 7 mm and 17 tests on 4 mm thick specimens. By comparing Figures 3 and 4, it can be seen that using the modified J instead of the deformation J, yields somewhat higher resistance curves. This agrees with the findings of Steenkamp (2). The difference however is only small, which is to be expected in view of the relatively low toughness of the material.

In Figure 5 the J_M-R curves for the SENT specimens are shown. Here the results are based on 6 tests on 2 mm and only 3 tests on 4 mm thick specimens. The reason is that a number of tests on 4 mm thick specimens were invalid because the specimen shifted relative to the test fixtures, thereby affecting the displacement measurement.

Effect of specimen geometry. It is clear that SENT specimens allow much larger crack extensions than SENB specimens. Within the crack extension range for the SENB specimens, the 4 mm curves shown in Figures 4 and 5 do not deviate significantly. This suggests that there is no effect of specimen geometry on the J_M-R curve.

Effect of nodule morphology. The results show that the J_M-R curves tend to be lower as the material thickness decreases. In view of the yield strength of the nodular cast iron, which is about 350 MPa, all crack extension occurred under plane stress conditions, irrespective of the specimen thickness. Thus, the changes in J_M-R curves must be caused by changes in nodule morphology. Rice and Johnson (6) developed a model for predicting the critical crack tip opening displacement (CTOD) necessary for crack extension in a material containing a void with diameter $2R_0$ at a distance X_0 straight ahead of the crack tip. Assuming the nodules mechanically behave like voids, critical J-values can be calculated for the current three nodule morphologies. For the 7, 4 and 2 mm thick material these values are 35, 19 and 8.4 N/mm. Clearly, the tendency is the same, namely a decreasing fracture toughness for smaller nodules which are closer to each other.

CONCLUSIONS

- Despite a crack front curvature in the SENB specimens that exceeded the amount permitted in the ASTM standard (1), it was found possible to obtain reliable crack length values using the compliance correction suggested by Steenkamp (2).
- J_M-R curves measured using the SENT geometry are not significantly different than those found for the standardised SENB geometry.
- As the thickness of the nodular cast iron decreases, and the nodules are smaller and closer together, the fracture toughness decreases. This is in accordance with a model presented by Rice and Johnson (6).

ACKNOWLEDGEMENTS

This work is performed within the framework of a business-oriented technology stimulation program (PBTS) of the Netherlands Ministry of Economic Affairs. Furthermore, the authors express their thanks to ir. P.C. van Eldijk of Hoogovens Research and Development, The Netherlands for his support.

REFERENCES

(1) ASTM Standard E 1152-95, "Standard Test Method for Determining J-R Curves", 1996 Annual Book of ASTM Standards, Vol. 03.01, ASTM, Philadelphia, USA, 1996, pp. 750-760.

(2) P.A.J.M. Steenkamp, "Investigation into the Validity of J-based Methods for the Prediction of Ductile Tearing and Fracture", Ph.D. thesis, Delft University of Technology, 1986.

(3) J.D. Landes, D.E. McCabe and H.A. Ernst, "Geometry Effects on the R-Curve", In: "Nonlinear Fracture Mechanics: Volume II - Elastic-Plastic Fracture", ASTM STP 995, eds. J.D. Landes, A. Saxena and J.G. Merkle, ASTM, Philadelphia, 1989, pp. 123-143.

(4) H.A. Ernst, "Material Resistance and Instability beyond J-Controlled Crack Growth", In: "Elastic-Plastic Fracture: Volume I-Inelastic Crack Analysis", ASTM STP 803, eds. C.F. Shih, J.P. Gudas, ASTM, Philadelphia, 1983, pp. 191-213.

(5) H. Tada, P.C. Paris and G.R. Irwin, "The Stress Analysis of Cracks Handbook", Del Research Corporation, Hellertown, 1973.

(6) J.R. Rice and M.A. Johnson, "The Role of Large Crack Tip Geometry Changes in Plane Strain Fracture", In: "Inelastic Behavior of Solids", eds. M.F. Kanninen, W.F. Adler, A.R. Rosenfield and R.I. Jaffee, McGraw-Hill, New York, 1969.

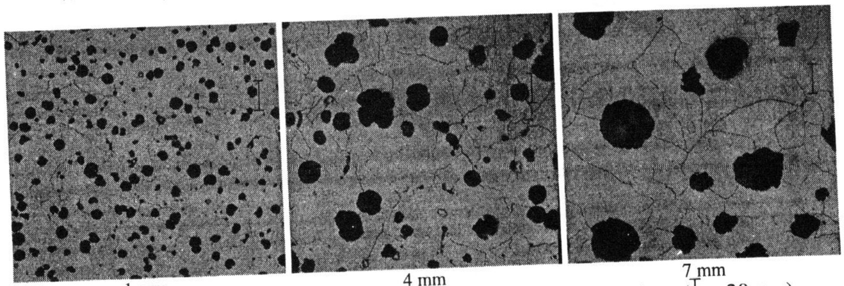

Figure 1 Metallographic structures of the investigated nodular cast iron (I = 20 μm)

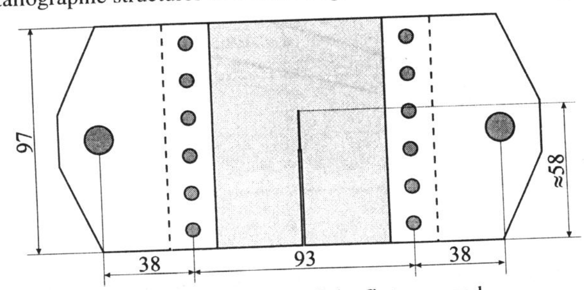

Figure 2 Geometry of the SENT specimen and the fixtures used

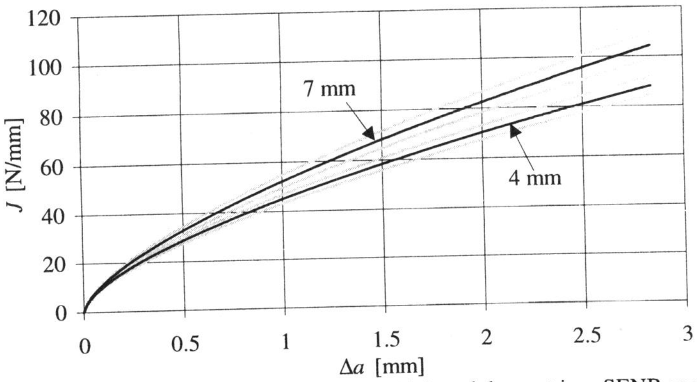

Figure 3 Average *J-R* curves for 7 and 4 mm thick nodular cast iron SENB specimens

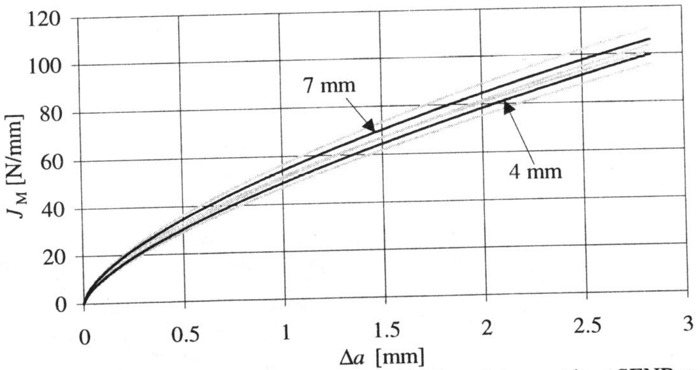

Figure 4 Average J_M-*R* curves for 7 and 4 mm thick nodular cast iron SENB specimens

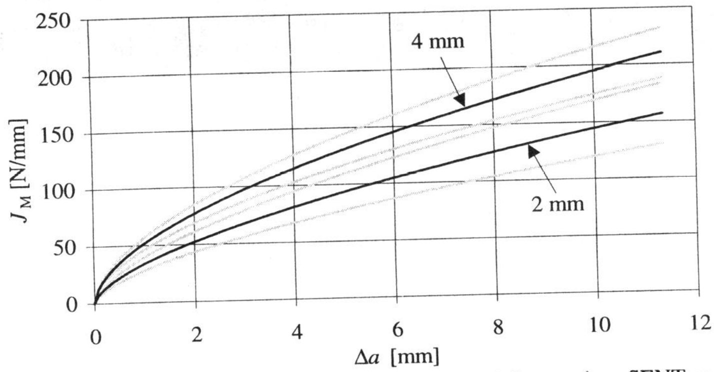

Figure 5 Average J_M-*R* curves for 4 and 2 mm thick nodular cast iron SENT specimens